ELSEVIER

Physica D 111 (1998) 335–346

PHYSICA D

Nonlinear dynamics of a single ferrofluid-peak in an oscillating magnetic field

Thomas Mahr *, Ingo Rehberg

Institut für Experimentelle Physik, Otto-von-Guericke-Universität, Postfach 4120, D-39016 Magdeburg, Germany

Received 13 December 1996; revised 14 February 1997; accepted 6 March 1997
Communicated by F.H. Busse

Abstract

If a magnetic field normal to the surface of a magnetic fluid is increased beyond a critical value a spontaneous deformation of the surface arises (normal field instability). The instability is subcritical and leads to peaks of a characteristic shape. We investigate the neighborhood of this instability experimentally under the influence of a temporal modulation of the magnetic field. We use a small vessel, where only one peak arises. The modulation can either be stabilizing or destabilizing, depending on the frequency and amplitude. We observe a cascade of odd-numbered response-periods up to period 11, and also a domain of even-numbered periods. We propose a minimal model involving a cutoff-conditon which captures the essence of the experimental observations.

PACS: 47.20.–k; 47.20.Ky; 75.50.Mm
Keywords: Magnetic fluid; Nonlinear oscillator; Subharmonic response; Surface instability

1. Introduction

Ferrofluids are colloidal suspensions of magnetic monodomains in a non-magnetic carrier liquid [1]. They behave like a super-paramagnetic substance, which allows for a wide range of applications [2], and a peculiar flow behavior under the influence of external magnetic fields [3–5]. In general the hydrodynamics of polarizable fluids is an interesting and non-trivial topic which includes such subtle effects as counter propagation of free surfaces under the influence of external magnetic fields [6,7]. Experimental investigations of the flow dynamics are hindered by the fact that the fluid is opaque. This seems to be the reason that investigations of the dynamic behavior of magnetic fluids are sparse, inspite of its tremendous technological potential [8]. We feel that investigations of dynamic surface deformations, which can be optically detected, are a practical approach to get a quantitative measurement of the flow behavior. In our experiment we drive nonlinear oscillations of the free surface of a ferrofluid by making use of the technical advantage that hydrodynamic motion can be induced by time dependent magnetic fields. The magnetic driving is particularly efficient in the neighborhood of static surface deforming instabilities, which can be achieved in super-paramagnetic fluids at relatively small external fields. These static instabilities are accompained by hysteresis leading to a particularly rich

* Corresponding author.
E-mail: thomas.mahr@physik.uni-magdeburg.de.

PII S0167-2789(97)00048-1

behavior of the nonlinear surface oscillations. Here we present an experimental investigation of such field induced surface deformations. The resulting bifurcation scenario of the nonlinear surface oscillations falls into a class which has never been studied experimentally. We discuss the results in terms of a qualitative model which captures the main features of the experimental findings.

2. Experimental setup and procedure

The experimental setup is shown in Fig. 1. In order to obtain a suitable compromise between viscosity and magnetic permeability, we use a mixture of the commercially available ferrofluids EMG 901 (Ferrofluidics) and EMG 909 in a ratio of 7 to 3. The properties of EMG 901 are: density $\rho = 1530\,\mathrm{Kg\,m^{-3}}$, surface tension $\sigma = 2.95 \times 10^{-2}\,\mathrm{Kg\,s^{-2}}$, initial magnetic permeability $\mu = 2.3$, magnetic saturation $M_S = 4.8 \times 10^4\,\mathrm{A\,m^{-1}}$, dynamic viscosity $\eta = 6 \times 10^{-3}\,\mathrm{N\,S\,m^{-2}}$. The properties of EMG 909 are: density $\rho = 1020\,\mathrm{Kg\,m^{-3}}$, surface tensiton $\sigma = 2.65 \times 10^{-2}\,\mathrm{Kg\,s^{-2}}$, initial magnetic permeability $\mu = 1.8$, magnetic saturation $M_S = 1.6 \times 10^4\,\mathrm{A\,m^{-1}}$, dynamic viscosity $\eta = 6 \times 10^{-3}\,\mathrm{N\,s\,m^{-2}}$. By assuming a linear interpolation for the fluid parameters of the mixture we obtain $\rho = 1377\,\mathrm{Kg\,m^{-3}}$, $\sigma = 2.86 \times 10^{-2}\,\mathrm{Kg\,s^{-2}}$, $\mu = 2.15$, $M_S = 3.84 \times 10^3\,\mathrm{A\,m^{-1}}$ and $\eta = 8.8 \times 10^{-3}\,\mathrm{N\,s\,m^{-2}}$. The critical field H_c for the onset of the normal field instability [1] has been measured to be $H_c = 6.2 \times 10^3\,\mathrm{A\,m^{-1}}$. This is in resonable agreement with the theoretical value $H_c = 5.9 \times 10^3\,\mathrm{A\,m^{-1}}$ calculated for infinite fluid layer. According to the same theory the critical wavelength is expected to be 9 mm. Due to aging of the fluid, presumably caused by evaporation of the carrier liquid, the critical field changes within one week by about 5%. The experimental runs shown below took on the order of hours, where aging effects can be estimated to be on the order of 0.1%.

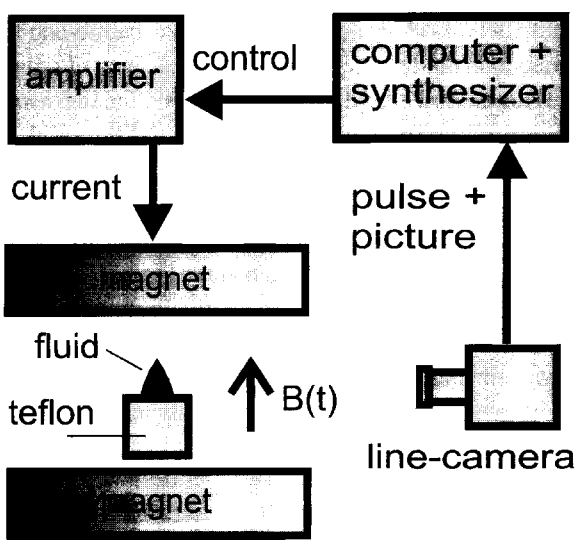

Fig. 1. Experimental setup.

The fluid is filled in a cylindrical teflon vessel of 12 mm depth and 3 mm diameter which is small in comparison to the critical wavelength of the normal field instability in a two-dimensional system and thus enforces the existence of a single peak. The upper 2 mm of the vessel has a slope with respect to the horizontal of 15°, which is close to the measured contact angle between fluid and teflon, in order to provide a flat surface of the fluid [9].

An image of the vessel is shown in Fig. 2, where two snapshots of the ferrofluid-peak are also presented, the first one taken at the phase of the oscillation where the amplitude reaches its minimum value, the second one taken at the maximum amplitude.

The vessel is placed in the center of a pair of Helmholtz-coils (Oswald), with an inner diameter of 40 cm. One coil consists of 474 windings of flat copper wire with a width of 4.5 mm and thickness 2.5 mm. A current of about 5 A is then sufficient to produce the magnetic field of about $8 \times 10^3\,\mathrm{A\,m^{-1}}$ used in this experiment. The static field is monitored by means of a hall probe (Group 3 DTM-141 Digital Teslameter) located below the vessel.

The dynamics of the ferrofluid surface is detected by a digital line scan camera (i2S iDC100) which is focused on the vertical axis through the center of the vessel. The time between two exposures is set to 6 ms.

The analysis of the lines is done with a 90 MHz Pentium-PC, equipped with a 6 bit interface board (i2S ISM197) for the line camera. The resolution in our experiment is 10.5 pixels per mm. For controlling

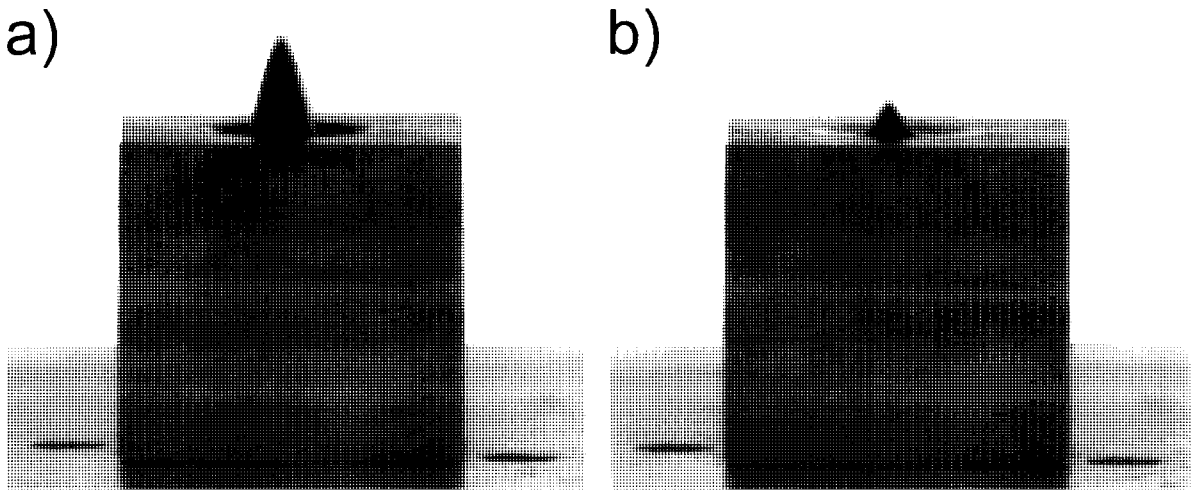

Fig. 2. Two snapshots of the ferrofluid-peak in the vessel. The first one is taken at the phase of the oscillation where the amplitude reaches its minimum value, the second one taken at the maximum amplitude.

the experiment the PC is also equipped with a synthesizer-board (WSB-10), and two programmable counters (8253), located on a multifunction I/O-board (Meilhaus ME-30). The counters are used to keep track of the pacing-frequency of the synthesizer-board. Their output is used to trigger the camera in any desired phase of the driving oscillation of the magnetic field. Thus we are using a phase-locked technique between the driving and the sampling in order to ensure a jitter-free measurement of the amplitude. By keeping track of the synthesizer pace the computer moreover manages the writing of the data into the synthesizer memory at times where no conflict with the DA-converter arises. This allows for smooth switching of the amplitude of the AC-component of the magnetic field. The wave-signal is amplified by a linear amplifier (fug NLN 5200 M-260). The resulting driving magnetic field is $H(t) = H_0 + \Delta H \sin 2\pi t f_D$, with H_0 as the static and ΔH as the oscillating part of the magnetic field; f_D is the driving frequency.

At constant driving frequency f_D and constant ΔH the static part H_0 is increased in constant steps. After a relaxation time of at least 5 s the minimum and maximum height is determined for each value of H_0. The response period T of the surface is analyzed by means of a correlation function.

3. Experimental results

We modulate a subcritical bifurcation by means of an oscillating magnetic field. The oscillation changes the character of this bifurcation. The subsequent oscillations of the surface can be harmonic, subharmonic or irregular depending on the magnitude of the static and the amplitude and frequency of the oscillating magnetic field. We condense the richness of the scenario into three phase-diagrams, using three representative driving frequencies. The most complex behavior is observed at a driving frequency of 13 Hz. The bifurcation diagrams simplify for smaller (larger) frequencies, for which we have taken 2.5 Hz (23.5 Hz) as a representative. These driving frequencies must be compared with the characteristic time of the system, which is given by the decay time of the peak once the field is turned off, and has been experimentally determined to be about 40 ms.

3.1. Modulating the subcritical bifurcation

Fig. 3 shows the height of the surface depending on the static field H_0 without modulation (a) and with modulation $\Delta H = 0.17\, H_c$ and $f_D = 13$ Hz (b). The unit of the magnetic field is the critical field $H_c =$

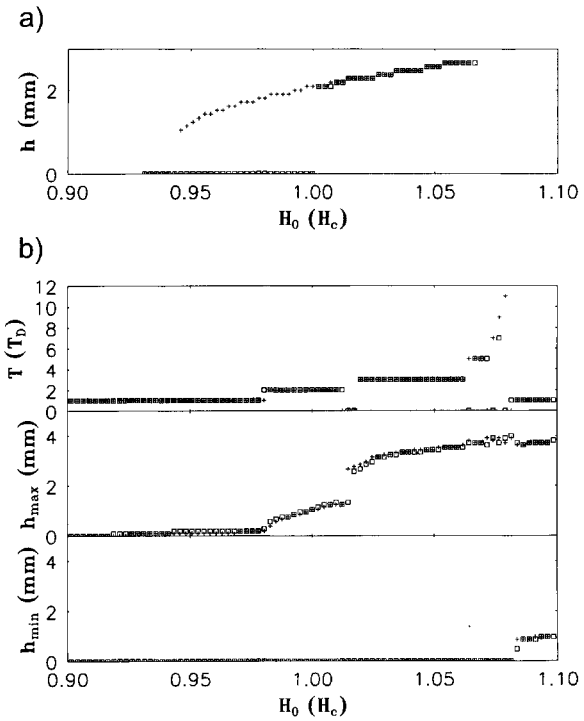

Fig. 3. (a) $\Delta H = 0$: Measurement of the height of the peak as a function of the static field H_0. (b) $\Delta H = 0.17H_c$: Measurement of the response-period T in units of the driving period T_D, and measurement of the maximum and minimum height. The driving period T_D is 76.16 ms. The upper part of each diagram corresponds to the minimum and maximum height of the peak in mm. Squares (crosses) correspond to the increasing (decreasing) field.

$6.2 \times 10^3\,\mathrm{A\,m^{-1}}$ of the normal field instability in the static case. The squares mark the increase of the static field and the crosses mark the adjacent decrease. Fig. 3(a) shows the hysteresis without field modulation. Starting with a flat surface and increasing the magnetic field leads to the onset of the normal field instability at $H_0 = H_c$, producing a peak of 2.1 mm height. Decreasing the field destroys the peak at the saddle–node field $H_s = 0.94H_c$.

In Fig. 3(b) the influence of the field modulation $\Delta H = 0.17H_c$ is presented. In order to characterize the different states of the surface, including subharmonic behavior, we need to observe the maximum height h_{max} and the minimum height h_{min} of the surface during a sufficiently large time period. Additionally the response period T in units of the driving period T_D is shown. If it is not possible to detect a periodic motion for a certain state, this state is marked with $T = 0$ in the diagram. We observe three qualitatively different oscillating states: The first is the flat surface, where $h_{min} = 0$ and $h_{max} = 0$. This state is labeled (0 0). It is measured for $H_0 < 0.92H_c$. For $H_0 > 1.08H_c$ the peak oscillates around its equilibrium height, that is $h_{min} > 0$ and $h_{max} > 0$. Therefore it is labeled (+ +). Between the flat surface and the oscillating peak lies a regime ($0.92H_c < H_0 < 1.08H_c$) where the peak periodically arises and collapses to zero height. We label this behavior (0 +). In this regime the dynamics of the surface is determined by the ratio of the driving period T_D to the characteristic times a peak needs to arise and collapse. This is the regime of interest where we observe complex temporal behavior, involving subharmonics as described below. At $H_0 = 0.92H_c$ the oscillating surface with response-period-1 develops softly from the flat surface. Deviations of h_{max} between the increasing and decreasing field are due to camera fluctuations. The period-1-states bifurcate at $H_0 = 0.98H_c$ into the period-2-states in a supercritical way. The transition from the period-2-states to the period-3-states at $H_0 = 1.015H_c$ shows a small hysteresis in the maximum height h_{max}. The coexisting period-2-attractor and period-3-attractor cause an irregualr motion. The peak then seems to change its mode in an intermittent way. Further increase of H_0 produces the odd-numbered subharmonic cascade 3–5–7–9–11. The single subharmonic states are separated by intermittent states. Further increase of H_0 leads to the (+ +)-state of the oscillating peak. We cannot exclude that the value of h_{max} is finite for $H_0 < 0.92H_c$. In this range the h_{max} is below our experimental resolution. We do indeed expect a finite value of h_{max} for any value of the driving field due to the spatial inhomogeneity of the magnetic field at the surface of the fluid.

The transition from the 1T to the 2T-mode is somewhat reminiscent of the observation reported for a long channel in [3]. In that case, as indicated by Fig. 1, the 2T-oscillation occurred in the form of a standing wave very reminiscent of the Faraday instability, i.e. a symmetric oscillation around the value $h = 0$ was

observed. In contrast, the 2T-mode of the single peak in our experiment oscillates around a finite positive value, and it appears via a period doubling bifurcation.

3.2. Dynamical behavior

An example of subharmonic behavior is demonstrated in Fig. 4, where we observe a response-period $T = 9T_D$. The ordinate corresponds to the actual height of the peak, while the abscissa indicates the time in units of the driving period. The time interval $1T_D$ consists of seven data points, which are linearly interpolated. Deviations in the periodicity of the measure are due to camera fluctuations.

3.3. Phase-diagrams $\Delta H(H_0)$

Figs. 5–7 describe the surface behavior by means of phase diagrams $\Delta H(H_0)$ at three different driving frequencies. For each value of ΔH the static part H_0 is increased starting at such values of H_0 for which the surface is still flat. The phase-diagrams are separated into the three domains (0 0), (0 +) and (+ +). The measured states of the flat (0 0)-domain are not marked with any color in the diagrams. But all states of the (0 +)-domain are shown in the diagrams by colors. In the (+ +)-domain only the onset-state for each value of ΔH is shown. The transition from (0 0) or (0 +) to (+ +)-modes is indicated by a dotted black line. Each figure consists of two parts: (a) shows the color-coded oscillatory mode and (b) shows the color-coded maximum height h_{max} of the surface. If it is not possible to identify a certain periodicity the number is replaced by the character 'I', because the peak then seems to change its subharmonic mode in an intermittent way.

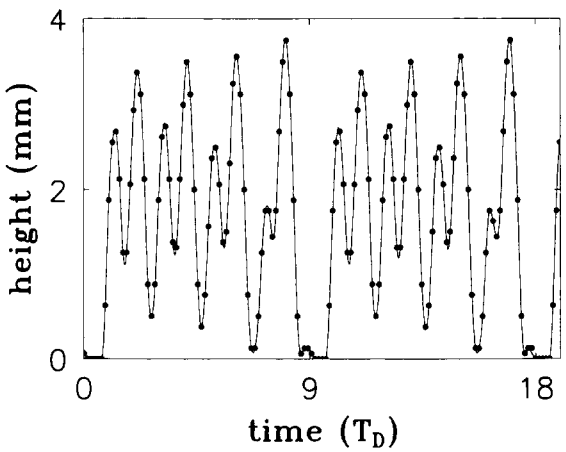

Fig. 4. The height of the peak during a time of 18 periods of excitation at $f_D = 13$ Hz. The solid line is obtained by a harmonic interpolation using the frequencies up to $3.5/T_D$, whose amplitude is determined by means of a discrete Fourier transformation. The time interval $1T_D$ consists of seven phase-locked sampled data points. Thus small deviations in the periodicity of the measure are presumably due to camera fluctuations. (For this measure we used a mixture of EMG 901 and EMG 909 in a ratio of 4 to 1, in contrast to the ratio of 7 to 3, in order to obtain a larger height of the peak.)

3.3.1. Low frequency

The results for low driving frequency $f_D = 2.5$ Hz are shown in Figs. 5(a) and (b). In the ΔH-range from 0 to 0.023 H_c we observe only two different states: the flat surface (0 0) and the oscillating peak (+ +). The threshold is decreased by modulation. For $\Delta H > 0.023H_c$ the (0 +)-domain is observed, but the response of the surface is always harmonic as can be seen in Fig. 5(a). The existence of three qualitatively different domains is due to the hysteresis of the static bifurcation. It can be understood in the quasi- static limit of $f_D \to 0$. Then we would expect the (0 0)-state if the total magnetic field grew up from zero but stayed always below H_c, (0 +)-modes if the driving field were below the saddle–node field H_s for a certain time of the period T_D, and (+ +)-modes if the driving field were always above the saddle–node field H_s. These two limit lines are drawn in Fig. 5(a): $\Delta H(H_0) = H_c - H_0$ (dashed line), $\Delta H(H_0) = H_0 - H_s$ (dashed–dotted line). Fig. 5(b) shows the maximum heights h_{max} of the peak. The higher H_0 the higher h_{max}, which is in accordance with the idea of the quasi-static limit.

3.3.2. Medium frequency

Fig. 6 shows the results for $f_D = 13$ Hz. For $\Delta H < 0.08H_c$ we measure only two different states, similar to the behavior at a frequency of 2.5 Hz: the flat surface (0 0) and the oscillating peak (+ +). The threshold is slightly increased by modulation in contrast to the

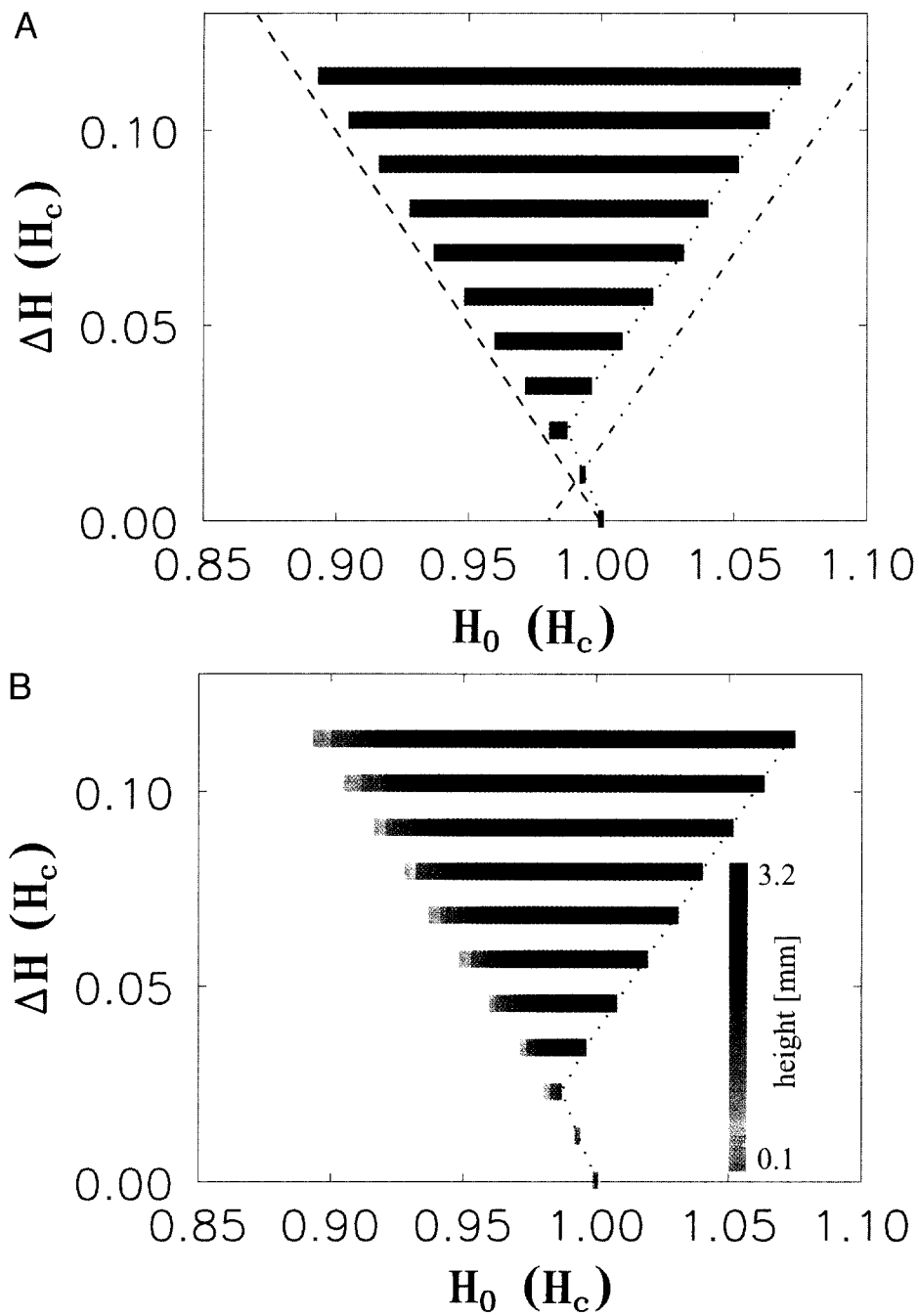

Fig. 5. Characterization of the measured surface dynamics depending on the increasing static field H_0 and the oscillating field ΔH at the low driving frequency $f_D = 2.5\,\mathrm{Hz}$; $H_c = 6.6 \times 10^3\,\mathrm{A\,m^{-1}}$. The transition from (0 0) or (0 +) to (+ +)-modes is indicated by a dotted line. (a) Only harmonic response is observed (green). Stationary limit: $\Delta H(H_0) = H_c - H_0$ (dashed line), $\Delta H(H_0) = H_0 - H_s$ (dashed–dotted line). (b) Coding of the maximum height.

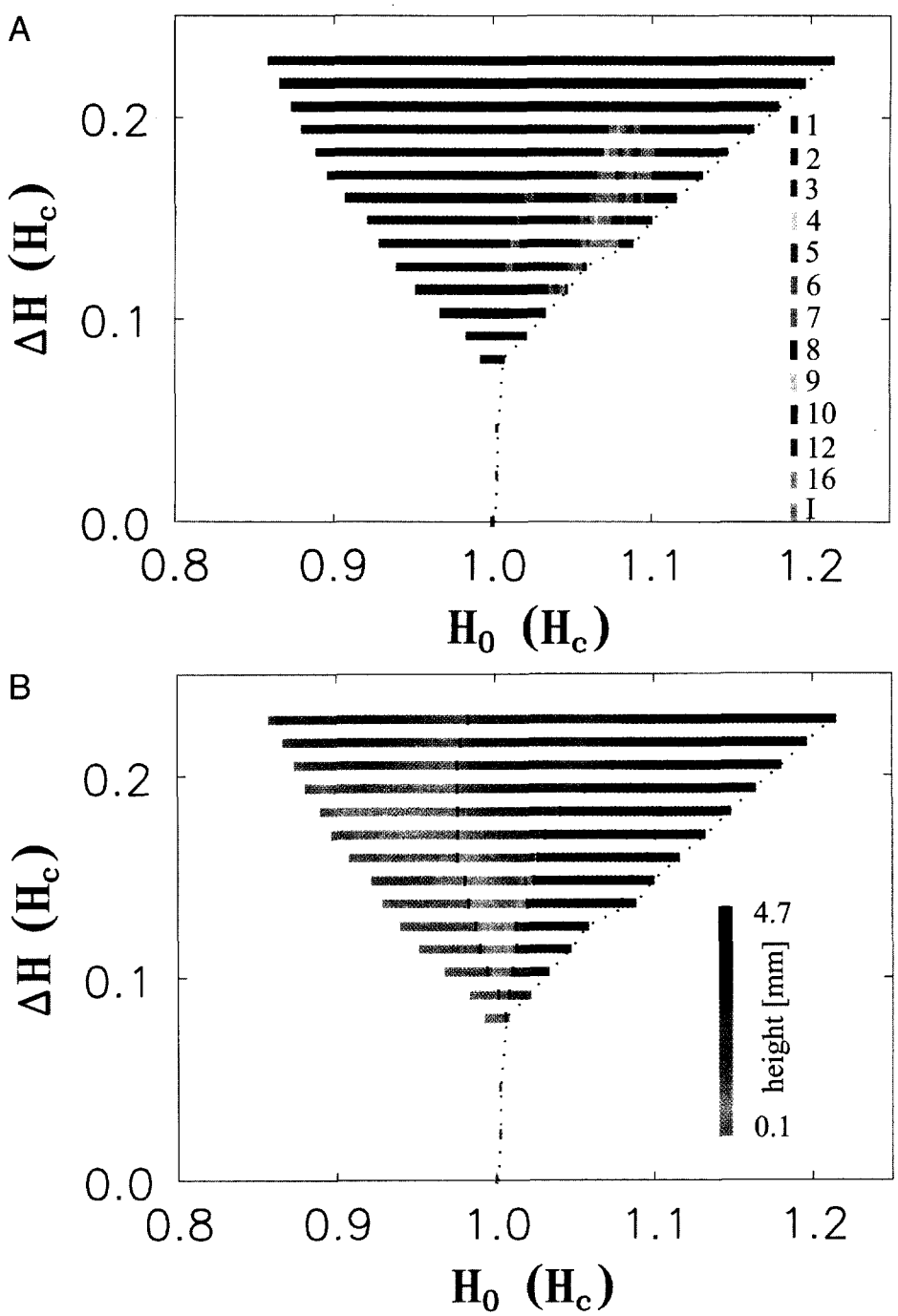

Fig. 6. Characterization of the measured surface dynamics depending on the increasing field H_0 and the oscillating field ΔH at the driving frequency $f_D = 13\,\mathrm{Hz}$; $H_c = 6.2 \times 10^3\,\mathrm{A\,m^{-1}}$. The transition from (0 0) or (0 +) to (+ +)-modes is indicated by a dotted black line. (a) Color-coding of the response period of the surface. The subharmonic cascade 1, 2, 3, 5, 7 and 9 T_D is observed. (b) Coding of the maximum height.

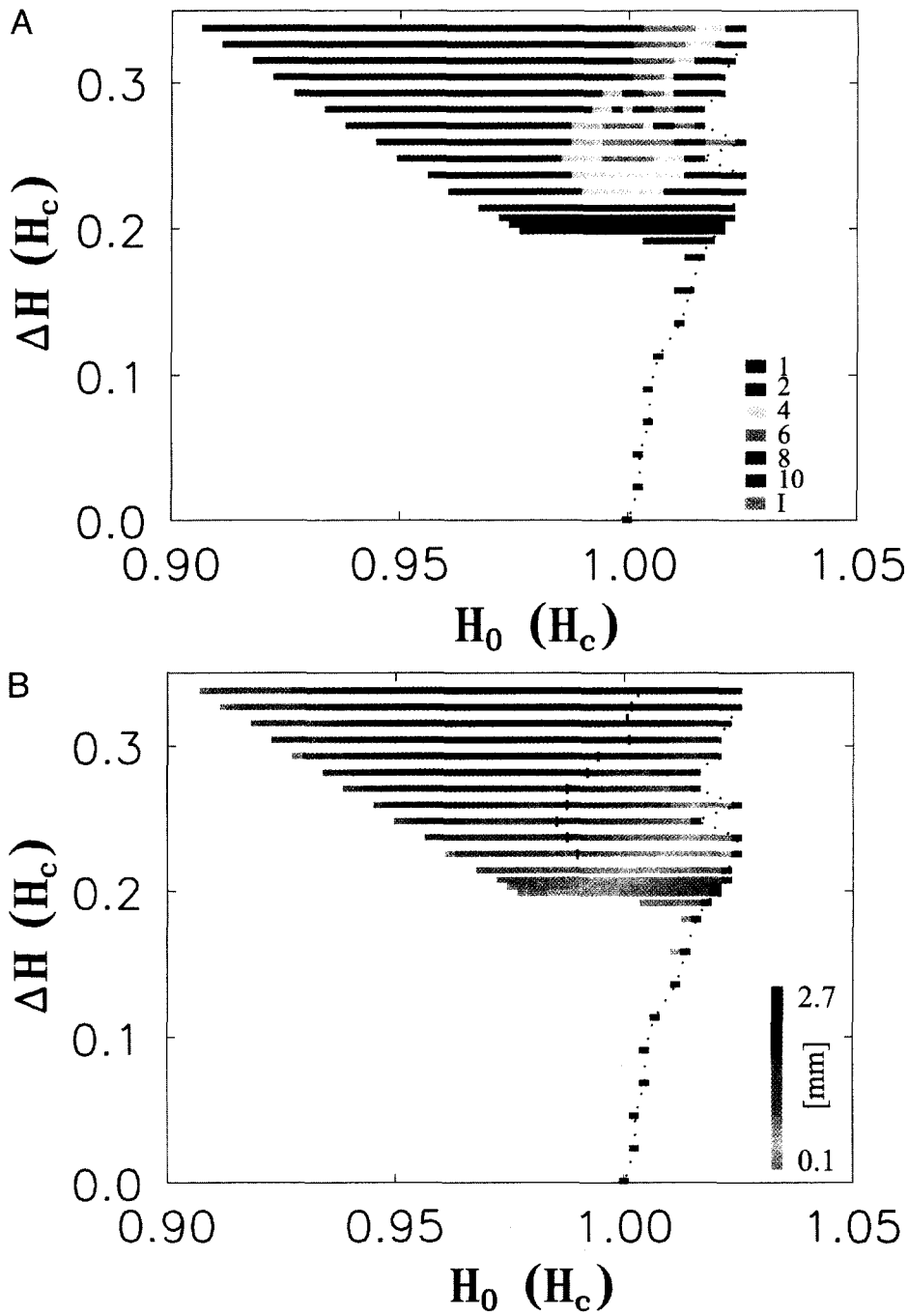

Fig. 7. Characterization of the measured surface dynamics depending on the increasing static field H_0 and the oscillating field ΔH at the driving frequency $f_D = 23.5\,\text{Hz}$; $H_c = 6.7 \times 10^3\,\text{A m}^{-1}$. The transition from (0 0) or (0 +) to (+ +)-modes is indicated by a dotted black line. (a) Color-coding of the response period of the surface. Only even-numbered subharmonic response is observed. (b) Coding of the maximum height.

measurement at 2.5 Hz. The ΔH-range of the direct transition between the two domains is also increased. For $\Delta H > 0.08 H_c$ there exists the (0+)-domain again, but now this domain has a fine-structure of different oscillatory modes as can be seen in Fig. 6(a). For low values of H_0 the surface response is harmonic. Increasing H_0 leads to a period-2-state. For sufficiently high oscillating fields, $\Delta H > 0.2 H_c$, and for high values of H_0 this state converts directly into the (++)-domain. But in the ΔH-range from 0.09 to 0.2 H_c we observe a 'balloon' of subharmonic and intermittent oscillations. For lower values of H_0 the odd-numbered subharmonic cascade of periods 3, 5, 7 and 9 T_D can be observed inside this balloon. These different states seem to be separated by intermittent states caused by coexisting attractors [10,11] of the pure states. While a period-1-state could softly bifurcate into a period-2-state, there exists no smooth transition from $T = 2$ to $T = 3$ and we observe irregular change of the dynamics between these attractors. The diagram shows that the basins of attraction are getting smaller for higher modes. For higher values of H_0 we can only observe intermittent states and the even-numbered subharmonic modes 4, 6, 8, 10, 12 and 16 within the balloon. A regular band-structure, like the odd-numbered cascade, of the even-numbered modes cannot be found in the phase-diagram. The maximum height h_{max} of the peaks is shown in Fig. 6(b). The transitions from period-1 to period-2, from period-2 to the balloon, and from the balloon to period-2 are indicated by small black bars. We observe, that some changes of the oscillating modes are connected with changes of h_{max}. At the transition point from period-1 to period-2 h_{max} is increased. The period-2 to period-3 transition also shown an increase of h_{max}. But in the small intermittent band between the period-2-states and the period-3-bands the height is decreased. There exist local maxima of h_{max} inside the period-1-band and the period-2-band, indicating the areas of strong reasonance of the oscillator.

3.3.3. High frequency

In Fig. 7 the results for high driving frequency $f_D = 23.5$ Hz are presented. The ΔH-range from 0 to 0.14 H_c, where we find only the flat surface and the domain with $h_{max} > 0$, is larger than in the case of 13 or 2.5 Hz. This can be understood, because in the case of $f_D \to \infty$ the fluid should not be influenced by the oscillating part. Therefore the (0+)-domain appears at higher values of ΔH for the high frequency $f_D = 23.5$ Hz. The threshold for the transition between the flat surface (0 0) and the (++)-domain is increased. For $\Delta H > 0.14 H_c$ we observe only even-numbered oscillating modes 2, 4, 6, 8 and 10, the period-1-state and the intermittent state as shown in Fig. 7(a). For low values of H_0 there exists only the period-2-state, except for two data points. The period-2-state changes into the period-4-state by a period-doubling-bifurcation in the ΔH-range from 0.23 to 0.29 H_c. For $\Delta H = 0.29 H_c$ the period-4-state is converted into a period-8-state if H_0 is increased. Inside the period-2 domain there exists a balloon again consisting of states with period 4, 6 and 8 T_D as well as intermittent states. The maximal height h_{max} is shown in Fig. 7(b). The transition from period-2 to period-4 or intermittency is again indicated by small black bars. Except for the area of the diagram described by high values of ΔH and low values of H_0 the height of the peaks is decreased if H_0 is increased, in contrast to the cases of lower driving frequencies f_D.

Even- and odd-numbered subharmonic responses are known from simulations of driven nonlinear oscillators [10,11]. Their range of existence is governed by the ratio of the driving period T_D to the natural period of the oscillator, which is in our case the time a peak needs to arise and collapse. In order to achieve a deeper understanding of the existence of the odd-numbered subharmonic cascade we derive a theoretical minimal model which reproduces the most striking observations of the bifurcation scenario.

4. Minimal model

We present a minimal theoretical model which captures the essence of the experimental findings, namely the existence of two oscillatory domains, the subharmonic dynamics, the hysteresis, the threshold shift and

the static behavior

$$\ddot{h} + \beta\dot{h} = h - h^2 + \epsilon(t),$$
$$\epsilon(t) = H_0 + \Delta H \sin 2\pi t/T_D - H_c$$

with a cutoff condition: $\dot{h}$ and h are set to zero if h reaches negative values. h represents the height of the peak and β measures the damping. We use a second derivative in the equation because the driving period is not very different from the characteristic times that a peak needs to arise and collapse. The force $h - h^2$ is the minimal form which considers the asymmetry of the system and which causes a hysteresis in connection with the cutoff condition. The additive coupling of the control parameter ϵ represents the magnetic field inhomogeneity caused by the magnetization of the fluid. Near the rim of the vessel, the field lines are not normal to the fluid surface. Thus, even small subcritical fields will lead to deformations of the fluid surface. Strictly speaking, the rising of the peak does not stem from a bifurcation and the additive coupling takes that into account. The cutoff condition is in accordance with the observation of very strong dissipative forces caused by the boundaries of the vessel when the peak breaks down.

Figs. 8(a) and (b) show the results of the numerical simulation for the parameters obtained from the fit explained below. At fixed driving the static part H_0 is increased from 0.7 to 1.2 H_c. For each value of H_0 the dynamic is determined after relaxation and is marked in the diagrams with a square. Crosses mark the adjacent decrease of H_0. Fig. 8(a) demonstrates the hysteresis of the static case without modulation. At $H_0 = H_c$ the solution $h = 0$ becomes unstable and the height h jumps to the fixpoint $h^*(\epsilon = 0) = 1$. Further increase of H_0 shifts the fixpoint to $h^*(\epsilon) = \sqrt{\epsilon + \frac{1}{4}} + \frac{1}{2}$. Decreasing H_0 leads to the saddle node $H_s = H_c - \frac{1}{4}$ where the finite solution becomes unstable. This dynamical behavior corresponds to the measured dynamic of Fig. 3(a). The influence of modulation is shown in Fig. 8(b). Starting again at the (0 0)-state at low values of H_0, the solution $h = 0$ becomes unstable in a supercritical way at $H_0 < H_c$. The response period of the (0 +)-state is $T = T_D$. By increasing H_0 this mode transforms supercritically into

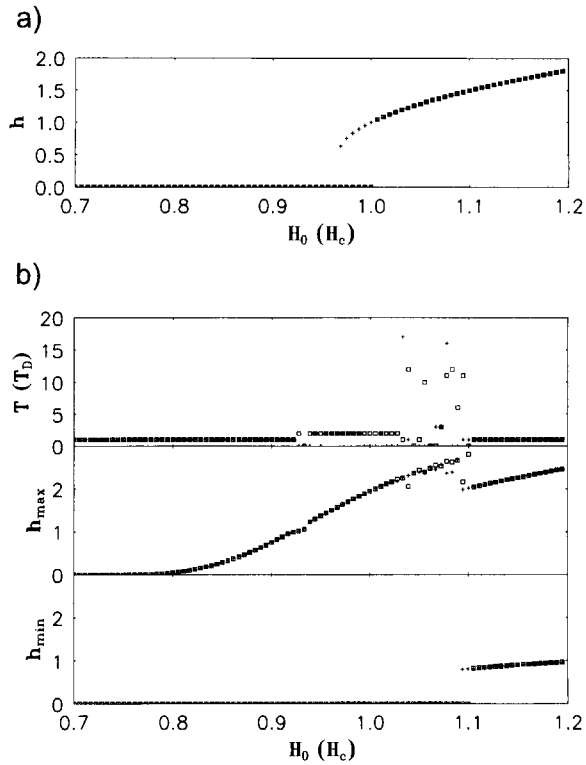

Fig. 8. Numerical simulation for the parameters obtained from the fit: (a) Height of the peak depending on the static field H_0 without modulation. (b) Minimum and maximum height of the peak and response period T depending on the static field H_0 at $\Delta H = 0.24 H_c$. Squares (crosses) correspond to the increasing (decreasing) field.

a period-2-state. Further increase of H_0 leads to higher subharmonic modes and intermittent states, which are marked in the diagram again with $T = 0$. For $H > 1.1 H_c$ the (+ +)-state becomes stable. A similar dynamic is observed in the experiment in Fig. 3(b). A decrease of H_0 shows no hysteresis except for some transitions in the subharmonic and intermittent regime.

In the model the exact transition from (0 0) to (0 +)-domains is always determined by the line $\Delta H(H_0) = H_c - H_0$, because then the resulting force $h - h^2 + \epsilon(t)$ is positive for a certain time. According to an experimental resolution limit of the height we introduce a threshold height h_{res} for the presentation of the simulations in the phase-diagram $\Delta H(H_0)$ of Fig. 9. The model-parameters β, T_D, H_c and h_{res} are used as fit-parameters to fit the numerical transition-line

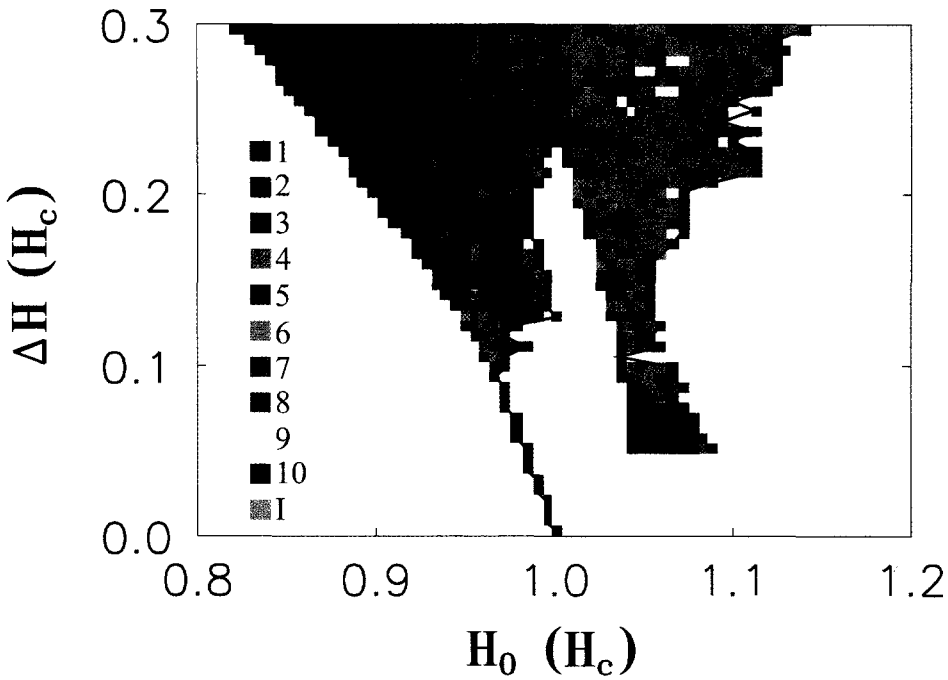

Fig. 9. Characterization of the surface dynamics obtained by numerical simulation for the parameters resulting from the fit. For each value of ΔH the static part H_0 is increased from 0.8 to 1.2 H_c. The response periods are shown by colors. The solid black line indicates the transition from (0 0) or (0 +) to (+ +)-modes. States lying on this line are already (+ +)-states.

(0 0) $\rightarrow$ (0 +) to the transition-line from the measurement at 13 Hz presented in Fig. 6 [12]. The initial parameters of each fit are chosen randomly from a certain interval. The best fits show good agreement with the measured transition-line (0 0) $\rightarrow$ (0 +), but the inner structure of the (0 +)-domain does not match with the measurements. Therefore in Fig. 9 there is presented the best fit, which shows an inner structure of the (0 +)-domain similar to the experimental data: $\beta = 0.07825422$, $T_D = 2.87910700$, $H_c = 7.48344946$ and $h_{res} = 0.4278$. The representation of the data is the same as in Figs. 5(a)–7(a), except for the label 'I', which marks periodic states with $T > 10T_D$ and states where no periodicity can be detected. The solid black line in Fig. 9 corresponds to the dotted black lines in Figs. 5–7, indicating the transition from (0 0) or (0 +) to (+ +)-modes. In the ΔH-range from 0 to 0.1 H_c the (0 0)-domain transforms directly into the (0 +)-domain. For $0.050H_c < \Delta H < 0.226H_c$ we observe that (+ +)-states can retransform into (0 +)-states in contradition to the experimental data shown before. Although this feature does not occur at all combinations of the model-parameters, we suppose that the retransformation could be suppressed by higher nonlinear terms. As in the experimental case referring to Fig. 6(a) we detect mainly the subharmonic cascade of response periods 1, 2, 3, 5, 7, 9 inside the (0 +)-domain for lower values of H_0. The period-2-regime includes a balloon of higher modes and intermittent states. The basins of attraction become smaller for higher modes in accordance with the experimental findings.

5. Summary and conclusion

We have studied the nonlinear surface oscillations of a magnetic fluid under the influence of a time dependent magnetic field in the neighborhood of a subcritical bifurcation. The nonlinear response involves

subharmonic regimes with periods up to 11 T_D, which are separated by regimes of irregular oscillations. At low frequencies the surface follows the frequency of the driving. At high frequencies only even-numbered subharmonics can be observed, while at medium frequencies a regime arises where odd-numbered subharmonics are dominant. These features are captured by a minimal model of the nonlinear oscillator.

We have used a harmonic driving $H(t) = H_0 + \Delta H \sin 2\pi t f_D$. It must be kept in mind that a time-periodic driving with different ratios of harmonics, i.e. square waves, will lead to quantitative differences in the bifurcation scenario. We have not performed a systematic study of those influences.

It seems to be interesting to study the interaction of many spatially coupled oscillating peaks. In the regime where subharmonic responses are favoured one would expect spatial domains with different phases of the oscillation. Thus experimental investigations in larger vessels are currently under way.

Acknowledgements

We would like to thank S. Linz and U. Parlitz for stimulating discussions. The experiments are supported by the 'Deutsche Forschungsgemeinschaft' through Re 588/10.

References

[1] R.E. Rosensweig, Ferrohydrodynamics (Cambridge University Press, Cambridge, 1993).
[2] R.V. Mehta, S.W. Charles and R.E. Rosensweig, Eds., Proc. Seventh Intern. Conf. on Magnetic Fluids, J. Magn. Mater. 149 (1995).
[3] J.-C. Bacri, U. d'Ortona and D. Salin, Phys. Rev. Lett. 67 (1991) 50.
[4] S. Sudo, M. Ohaba, K. Katagiri and H. Hashimoto, J. Magn. Magn. Mater. 122 (1993) 248.
[5] F. Elias, C. Flament and J.-C. Bacri, Phys. Rev. Lett. 77 (1996) 643.
[6] R.E. Rosensweig, Science 271 (1996) 614.
[7] M. Liu, Phys. Rev. Lett. 70 (1993) 3580.
[8] V.E. Fertman, Magnetic Fluids: Guidebook (Hemisphere, New York, 1990).
[9] T. Mahr, A. Groisman and I. Rehberg, J. Magn. Magn. Mater. 159 (1996) L45–L50.
[10] C. Scheffczyk, U. Parlitz, T. Kurz, W. Knop and W. Lauterborn, Phys. Rev. A 43 (1991) 6495.
[11] R. Mettin, U. Parlitz and W. Lauterborn, Int. J. Bifur. and Chaos 3 (1993) 1529.
[12] W.H. Press, B.P. Flannery, S.A. Teukolsky and W.T. Vetterling, Numerical Recipes in C (Cambridge University Press, Cambridge, 1992).